

Potential use of *Momordica charantia* (bitter gourd) waste as a low-cost adsorbent to remove toxic crystal violet dye

Linda B.L. Lim^{a,*}, Namal Priyantha^{b,c}, Ke Jia Mek^a, Nur Afiqah Hazirah Mohamad Zaidi^a

^aDepartment of Chemistry, Faculty of Science, Universiti Brunei Darussalam, Jalan Tungku Link, Gadong, Negara Brunei Darussalam, Tel. 00-673-8748010, email: linda.lim@ubd.edu.bn (L.B.L. Lim), mek_ke_jia@hotmail.com (K.J. Mek), afhazirah@gmail.com (N.A.H.M. Zaidi)

^bDepartment of Chemistry, Faculty of Science, University of Peradeniya, Peradeniya, Sri Lanka

^cPostgraduate Institute of Science, University of Peradeniya, Peradeniya, Sri Lanka, namal.priyantha@yahoo.com (N. Priyantha)

Received 5 March 2017; Accepted 8 June 2017

ABSTRACT

Momordica charantia (bitter gourd) waste (BGW) was investigated for its potential as an adsorbent in removing crystal violet (CV) dye. Batch adsorption isotherm studies analyzed using six isotherm (Langmuir, Freundlich, Temkin, Dubinin-Radushkevich, Redlich-Peterson and Sips) models showed that both the Langmuir and Sips models fitted well to the experimental data, with the Langmuir-model giving a higher R^2 (0.9924) than Sips (0.9899) but the Sips model having lower overall error values. The maximum adsorption capacity (q_{max}) of BGW for CV dye is 244.8 mg g⁻¹ (Sips) and 261.8 mg g⁻¹ (Langmuir), demonstrating BGW is a good adsorbent as compared to many reported adsorbents. Further, adsorption of CV on BGW is exothermic and spontaneous in nature, with an average ΔH° of -10.2 kJ mol⁻¹. Except at pH 2, BGW was able to adsorb CV at higher medium pH with >80% removal. The pseudo second order kinetics model fitted the adsorption of CV with R^2 close to unity for all the three concentrations of CV tested. Performance of BGW toward CV removal was affected by the presence of salt, with NaCl being the most influential as compared to KCl and KNO₃. Regenerated spent BGW still maintained excellent CV adsorption even after the 5th cycle, removing 82% and 96% CV using acid and base treatment respectively, further supporting the strong potential of BGW as a low-cost adsorbent.

Keywords: *Momordica charantia* (bitter gourd) adsorbent; Adsorption isotherm; Cationic crystal violet dye; Regeneration

1. Introduction

In this era of modernization, more industries are being developed in order to meet the demands of the growing population. With the increase of industries over the past few decades, the amounts of pollutants that are being released to the environment are on the rise as well, thereby causing serious hazardous pollution. Due to synthetic dyes being commercially available, less expensive and having a wider variation of colors, industries now turn to the use synthetic dyes in textile, food, cosmetic and dyeing plastic, rubber, paper, leather materials. As a

result, these industries are now the main contributor to the water pollution.

Utilization of adsorption technique to clean up pollutants such as heavy metals and dyes has gained increasing popularity over the past decade [1–3]. The reasons lie in its simplicity and straight forwardness, and more importantly it is low cost and effective compared to many other techniques. As a result, many adsorbents have been used and these include peat [4–6], aquatic plants [7–10], fruit wastes [11–13], leaves [14,15], stem [16], synthetic materials [17–21], wastes from agriculture [22–24] and industries [25,26], and many others [27–37].

*Corresponding author.

Crystal violet (CV) dye, otherwise known as methyl violet 10 B or gentian violet, is commonly used in medicines as it has antibacterial, antifungal, antiangiogenic, antitrypanosomal, antitumor and antihelminthic properties [38,39]. Although CV is not used as a textile dye, it is used to dye paper, and as a marker to locate the piercing on body. It has been shown that CV has carcinogenic effects in organs of mice as well as carcinogenic and mutagenic effects in rodents [40]. Cancer in the digestive tracks in animals has also been linked to this dye [41,42]. Further, CV has not been proven to be a safe animal feed by the Food and Drug Administration (FDA) in the United States of America.

Momordica charantia, also known as Bitter gourd or Bitter melon, belongs to the family of Cucurbitaceae. They are widely grown in Asia. In Brunei Darussalam, bitter gourds are normally eaten as a vegetable dish. Despite its bitter taste, bitter gourd is popular as it has various health benefits. The flesh is eaten while the pith and seeds are thrown away as wastes. To date, literature on the use of Bitter gourd as a natural adsorbent is limited. Munichandran et al. reported the use of the seeds for the removal of heavy metals (nickel and lead) [43]. Bitter gourd peroxidases have been reported to be highly effective in decolorizing textile dyes [44] as well as in removing phenols [45] and anthracene [46]. Surprisingly, no information on the use of bitter gourd waste from pith and seeds (BGW) is available for the removal of dyes. Hence, to investigate the feasibility of BGW as a potential natural low-cost adsorbent, the present study focuses on the use of BGW for the removal of CV dye. To the best of our knowledge, this is the first report on the use of BGW for the removal of this dye.

2. Materials and methods

2.1. Sample preparation and chemical reagents

Bitter gourds were randomly bought from the local market. The inedible part, which consisted of the seeds and pith, normally discarded as waste, was separated from the edible part and dried in an oven at 80°C until a constant mass was obtained. Thereafter, the dried bitter gourd wastes (BGW) were blended and sieved using laboratory metal sieves to obtain the desired particle size of < 355 µm which was used throughout this study. Crystal violet (CV) of > 90% purity [molecular formula of $C_{25}N_3H_{30}Cl$, molecular weight of 407.979 g mol⁻¹] was purchased from Sigma-Aldrich and used without further purification.

2.2. Adsorption studies

Investigation of the effects of contact time (0–240 min), pH (2–0) and ionic strength (0–1 mol dm⁻³ salt) on the extent of adsorption, and batch experiments for both adsorption isotherm and kinetics were carried out following the methods as described by Dahri et al. with slight modification [47]. Investigation into adsorption

mechanism was carried out using CV of concentrations 100, 500 and 700 mg L⁻¹ at room temperature. Thermodynamics studies were done within the temperature ranging from 298 to 343 K. The mixture of adsorbent-CV solution was agitated at room temperature using the Stuart Scientific Flask Shaker SF1 set at the speed of 250 rpm. All experiments were carried out in duplicate, unless otherwise stated. The point of zero charge of BGW was determined using method as described by Lim et al. [48]. The Shimadzu, UV-1601PC spectrophotometer was used to measure the absorbance of CV dye at the wavelength of 590 nm. Regeneration studies were carried out according to the procedure as laid out by Chieng et al. [49] with slight modification.

3. Results and discussion

3.1. Effect of contact time

Investigation of the contact time required for the adsorbent-adsorbate system to reach equilibrium was carried out using CV dye, as described by Kooh et al. [50]. With 100 mg L⁻¹ CV dye, the results (Fig. 1) show that BGW is able to remove > 98% of the dye within 30 min. When a higher dye concentration of 1000 mg L⁻¹ CV was used, contact time period of 210 min was determined to be sufficient. A rapid increase in the removal of CV was observed within the first 30 min, attributing to the availability of vacant sites on the surface of BGW for the adsorption of dye. As time progresses, more and more CV dyes occupy these active sites, causing the adsorption rate to decrease, and eventually an equilibrium is reached. All subsequent experiments were carried out using contact time of 210 min to ensure full equilibrium has been reached.

3.2. Effect of medium pH and BGW's point of zero charge

At its untreated pH (6.53), a removal of 85.8% of CV dye was observed (Fig. 2). Above this pH, there is a very

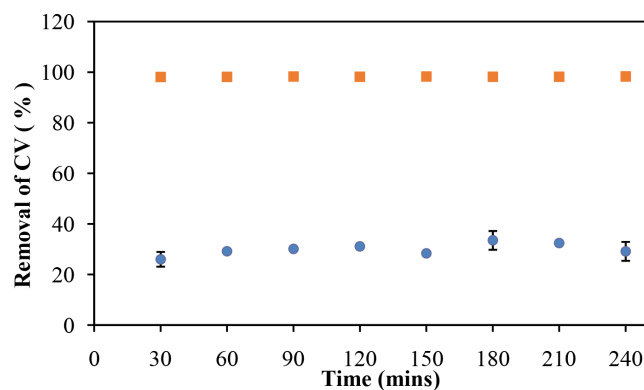


Fig. 1. Contact time required for the BGW-CV system to reach equilibrium [mass of BGW = 0.050 g; volume of CV solution = 25 mL; concentrations of CV = 100 (■) and 1000 (●) mg L⁻¹].

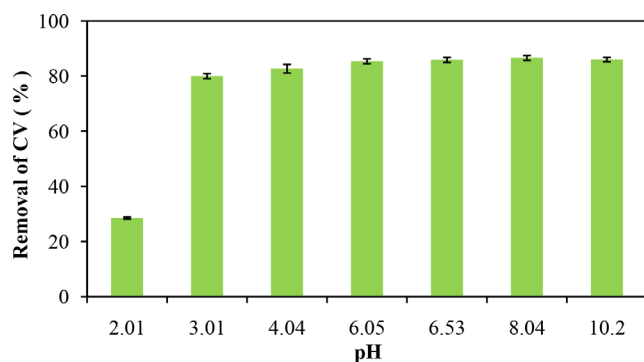


Fig. 2. Adsorption of CV onto BGW in different medium pH [mass of BGW = 0.050 g; volume of CV solution = 25 mL; concentration of CV = 100 mg L⁻¹].

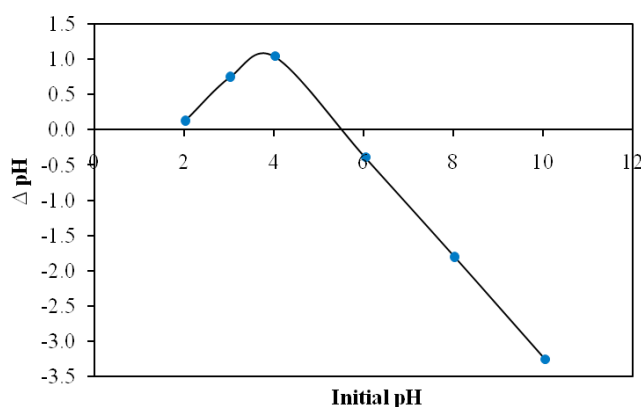


Fig. 3. Change in pH as a function of initial pH to determine the point of zero charge (pH_{pzc}) of BGW [mass of BGW = 0.050 g; volume of solution = 25 mL].

slight difference of less than 1%, while at lower pH, there is a noticeable decrease in removal of CV. However, a good removal of CV was still maintained at pH 3 (80%). Under strong acid medium (pH 2), a drastic decrease of 57% in dye removal was observed. This is probably due to protonation of the nitrogen atoms of the dye molecule which then competes with large amount of H⁺ ions present in solution for the active sites on the adsorbent's surface. Hence, in this study, medium pH was maintained above 2. Further, at pH 2, the surface of BGW is expected to be predominantly positive in charge since this pH is lower than the point of zero charge (pH_{pzc}) of BGW determined to be 5.5 (Fig. 3). This in turn will result in electrostatic repulsion between the cationic dye and the positively charged surface, thereby reducing the amount of CV being adsorbed onto the surface. The pH_{pzc} is the pH at which the surface of an adsorbent has zero charge. At $\text{pH} > \text{pH}_{\text{pzc}}$, a slight improvement of the removal of CV was observed whereby the adsorbent's surface is expected to be predominantly negative in charge, thus enhancing interactions with the cationic dye molecules. Since adsorption of CV at untreated pH (85.8%) was high and exhibited only 1% difference in removal to its

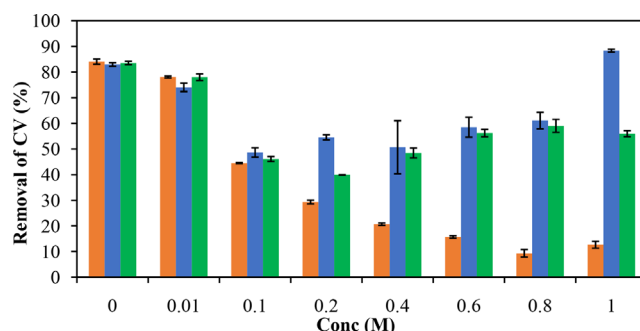


Fig. 4. Effect of ionic strength using NaCl (■), KNO₃ (■) and KCl (■) [0.050 g of BGW; 25 mL of 100 mg L⁻¹ CV solution].

maximum pH at 8 (86.6%), no adjustment of medium pH was deemed necessary. Hence throughout the rest of the adsorption experiments, untreated pH medium was used.

3.3. Effect of ionic strength

Three different salts (NaCl, KCl and KNO₃) were investigated for their effects on the adsorption of CV dye by BGW and studies were carried out from concentration ranging from 0 to 1 M. Of these three salts, NaCl showed the highest effect whereby an approximately 70% reduction in the adsorption of CV by BGW was observed when the salt concentration was increased from 0 to 1 M (Fig. 4). Both KCl and KNO₃ exhibited similar trends where there was an initial decrease in reduction in dye removal which was followed by a steady increase beyond 0.4 M. Unlike NaCl, the maximum decrease in adsorption of CV dye was 34% and 44% at 0.1 M KNO₃ and 0.2 M KCl, respectively. Reduction in dye adsorption could be the result of competition between metal ions with cationic CV dyes for a limited number of adsorption sites on the surface of BGW. One possible explanation for the greater effect of NaCl on adsorption could be due to Na⁺ ions, being smaller in size, could occupy the surface active sites better.

3.4. Adsorption isotherm

Batch adsorption isotherm experiments were carried out for the adsorption of CV onto BGW at room temperature using CV dye concentrations ranging from 0 to 1000 mg L⁻¹. The experimental data obtained were fitted to six adsorption isotherm models namely Langmuir [51], Freundlich [52], Dubinin-Radushkevich (D-R) [53], Temkin [54], Redlich-Peterson (R-P) [55] and Sips [56] models. Their linearized equations and the corresponding linear plots are shown in Table 1. These models have been widely discussed in various literature. Briefly, the Langmuir model applies to homogenous surface of adsorbent to complete a monolayer. The Freundlich model describes adsorption of adsorbates on a heterogeneous surface that can extend up to many layers, while R-P is a three parameter model which combines

Table 1
Linearized isotherm models used and their corresponding linear plots

| Isotherm model | Linearized equation | Plot |
|----------------------------|---|---|
| Langmuir | $\frac{C_e}{q_e} = \frac{1}{K_L q_{\max}} + \frac{C_e}{q_{\max}}$ K_L is the Langmuir constant | $\frac{C_e}{q_e}$ vs C_e |
| Freundlich | $\log q_e = \frac{1}{n} \log C_e + \log K_F$ K_F is the Freundlich constant indicative of adsorption capacity; n is related to the adsorption intensity | $\log q_e$ vs $\log C_e$ |
| Temkin | $q_e = \left(\frac{RT}{b_T} \right) \ln K_T + \left(\frac{RT}{b_T} \right) \ln C_e$ K_T is the Temkin constant; b_T is related to the heat of adsorption; R is the gas constant while T is the absolute temperature at 298 K | q_e vs $\ln C_e$ |
| Dubinin-Radushkevich (D-R) | $\ln q_e = \ln q_{\max} - \beta \epsilon^2$ where β is D-R constant and Polanyi potential (ϵ) = $RT \ln \left(1 + \frac{1}{C_e} \right)$ Mean free energy (E) = $\frac{1}{\sqrt{2\beta}}$ | $\ln q_e$ vs $-\beta \epsilon^2$ |
| Redlich-Peterson (R-P) | $\ln \left(\frac{K_R C_e}{q_e} - 1 \right) = n \ln C_e + \ln a_R$ K_R and a_R are the R-P constants | $\ln \left(\frac{K_R C_e}{q_e} - 1 \right)$ vs $\ln C_e$ |
| Sips | $\ln \left(\frac{q_e}{q_{\max} - q_e} \right) = \frac{1}{n} \ln C_e + \ln K_s$ K_s is the Sips constant; n is the Sips exponent | |

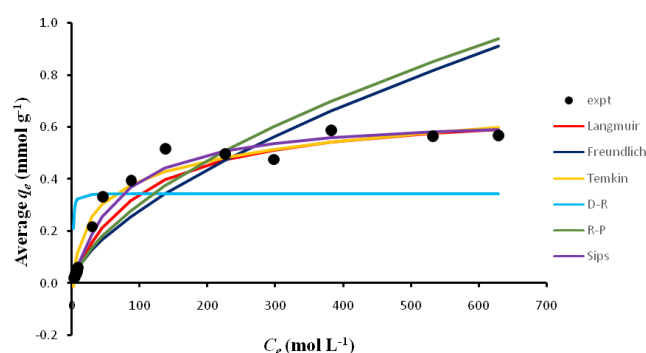


Fig. 5. Comparison of simulation plots of various isotherm models with experimental data [mass of BGW = 0.050 g; volume of CV solution = 25 mL; concentration of CV = 0–1000 mg L⁻¹]

both the Freundlich and Langmuir isotherm models, tending toward Freundlich at high adsorbate concentrations. According to the Temkin model, due to the uniform distribution of the binding energies, there is a linear decrease of

heat of adsorption with increasing surface coverage. The D-R model postulates pore-filling, not layer-by-layer surface coverage, and thus adsorption occurs in micropores. Similar to the R-P model, the Sips model is also a three-parameter model, combining both the Freundlich and Langmuir models, which reduces to the Langmuir model at high adsorbate concentrations.

The regression coefficient (R^2) values of the linearized isotherm plots, as shown in Table 2, in decreasing order is as follows: Langmuir > Sips > Temkin > Freundlich > D-R > R-P. Simulated plots, as shown in Fig. 5, is also in line with this observation where the last three isotherm models are clearly deviated from the experimental isotherm data, thereby indicating their unsuitability to describe the adsorption of CV on BGW.

It has been shown that there is a possibility of violating error variance and standard least square normality assumptions when equations of non-linear isotherms are transformed to corresponding linear forms [57,58]. Hence, in order to further confirm the best fit adsorption isotherm model for this study, error analyses were performed using four error functions as shown in Eqs. (1)–(4) below.

Table 2
Adsorption isotherm parameters for different models and their error values

| Model | Values | ARE | SSE | EABS | χ^2 | HYBRID |
|--|----------|--------|-------|-------|----------|--------|
| Langmuir | | 8.47 | 0.008 | 0.296 | 0.030 | 0.20 |
| q_{max} (mg g ⁻¹) | 261.84 | | | | | |
| K_L (L mmol ⁻¹) | 0.01 | | | | | |
| R^2 | 0.9924 | | | | | |
| Freundlich | | 19.17 | 0.123 | 0.963 | 0.281 | 1.87 |
| K_F (mmol g ⁻¹ (L mmol ⁻¹) ^{1/n}) | 0.02 | | | | | |
| n | 1.69 | | | | | |
| R^2 | 0.9411 | | | | | |
| Temkin | | 23.25 | 0.013 | 0.417 | 0.143 | 0.96 |
| K_T (L mmol ⁻¹) | 0.19 | | | | | |
| b_T (kJ mol ⁻¹) | 19.36 | | | | | |
| R^2 | 0.9809 | | | | | |
| Dubinin-Radushkevich | | 259.10 | 1.010 | 3.54 | 14.22 | 94.78 |
| q_{max} (mg g ⁻¹) | 184.04 | | | | | |
| B (J mol ⁻¹) | 1.36E-06 | | | | | |
| E (kJ mol ⁻¹) | 0.61 | | | | | |
| R^2 | 0.9000 | | | | | |
| Redlich-Peterson | | 18.52 | 0.118 | 0.943 | 0.270 | 1.93 |
| K_R (L mol ⁻¹) | 0.10 | | | | | |
| a | 0.42 | | | | | |
| a_R (L mmol ⁻¹) | 4.72 | | | | | |
| R^2 | 0.8920 | | | | | |
| Sips | | 5.79 | 0.003 | 0.173 | 0.013 | 0.09 |
| q_{max} (mg g ⁻¹) | 244.79 | | | | | |
| K_S (L mmol ⁻¹) | 0.01 | | | | | |
| $1/n$ | 1.16 | | | | | |
| n | 0.87 | | | | | |
| R^2 | 0.9899 | | | | | |

Table 3
Adsorption capacity (q_{max}) values of BGW and selected reported adsorbents

| Adsorbent | q_{max} (mg g ⁻¹) | Reference |
|---|---------------------------------|------------|
| Bitter gourd waste | 244.8 (Sips) | This study |
| | 261.8 (Langmuir) | This study |
| <i>Artocarpus altilis</i> (breadfruit) skin | 150.1 (Sips) | [59] |
| | 145.8 (Langmuir) | |
| <i>Artocarpus odoratissimus</i> (Tarap) skin | 118 | [60] |
| NaOH treated <i>Artocarpus odoratissimus</i> skin | 195 | [60] |
| <i>Artocarpus odoratissimus</i> leaf | 50.5 | [61] |
| <i>Artocarpus heterophyllus</i> (Jackfruit) leaf | 43.4 | [62] |
| <i>Artocarpus camansi</i> (Breadnut) skin | 275 | [63] |
| NaOH treated <i>Artocarpus camansi</i> skin | 479 | [63] |
| Yeast-treated peat | 18.0 | [64] |
| <i>Parkia speciosa</i> (Petai) pod | 163.2 | [65] |
| Functionalized cellulosic microfibers | 872.0 | [66] |
| Date stone | 90.9 | [67] |
| Activated carbon | 19.8 | [68] |
| Magnetite/silica/pectin Nanoparticles | 180.3 | [69] |
| Magnetite/pectin nanoparticles | 149.5 | [69] |
| Peat | 108.0 | [70] |
| Coniferous pinus bark powder | 32.8 | [71] |
| Alginate acid/activated bentonite | 582.4 | [72] |
| Grapefruit peel | 254.2 | [73] |
| Acidic fly ash | 9.2 | [74] |

$$\text{Sum square error (SSE): } \sum_{i=1}^n (q_{e,calc} - q_{e,meas})_i^2 \quad (1)$$

Hybrid fractional error function (HYBRID)

$$\frac{100}{n-p} \sum_{i=1}^n \left[\frac{(q_{e,meas} - q_{e,calc})^2}{q_{e,meas}} \right]_i \quad (2)$$

$$\text{Sum of absolute error (EABS): } \sum_{i=1}^n |q_{e,meas} - q_{e,calc}| \quad (3)$$

$$\text{Chi-square } (\chi^2): \sum_{i=1}^n \frac{(q_{e,meas} - q_{e,calc})^2}{q_{e,meas}} \quad (4)$$

where $q_{e,meas}$ is the experimental adsorption capacity at equilibrium, $q_{e,calc}$ is the calculated adsorption capacity at equilibrium, n is the number of data points in the experiment and p is the number of parameters in the model.

Even though the Temkin isotherm model provides simulation data close to the experimental data with a reasonably good R^2 , it has the second largest overall error values. Hence, this model will not be considered further to account for adsorption of CV. Of the two remaining isotherm models, despite the R^2 of the Langmuir model being higher than that of the Sips model, the simulation plots show that the Sips model has a closer fit to the experimental isotherm as compared to the Langmuir model. This is further confirmed by the overall lower error values of the Sips model, indicating that this model better describes the adsorption of CV on BGW. Based on the Sips model, the maximum adsorption capacity (q_{max}) of BGW is 244.79 mg g⁻¹ while the Langmuir model gives a comparable q_{max} of 261.84 mg g⁻¹.

The adsorption capacity of BGW is superior to many low-cost adsorbents such as wastes from different types of *Artocarpus spp.*, and many others including activated carbon and synthesized nanoparticles, as shown in Table 3.

Its q_{max} is comparable to breadnut and grapefruit peel. Further improvement on adsorption capacity would be highly likely after a surface modification step.

3.5. Thermodynamic studies

Thermodynamics of the adsorption process was investigated using three different CV dye concentrations (100 mg L⁻¹, 300 mg L⁻¹ and 500 mg L⁻¹). Thermodynamics parameters determined based on Eqs. (5)–(8) with the aid of the plot of $\ln K$ vs. $1/T$ indicate that the adsorption process is exothermic in nature with standard enthalpy change (ΔH°) being negative (Fig. 6, Table 4). The negative standard Gibbs free energy change (ΔG°) values suggest that the adsorption process is favorable and spontaneous. Increase in temperature of adsorption from 298 K to 343 K leads to negative standard the entropy (ΔS°) values for all the three concentrations of CV dyes investigated, suggesting that there may be an increase orderliness in the system.

$$\text{Van't Hoff equation: } \Delta G^\circ = \Delta H^\circ - T\Delta S^\circ \quad (5)$$

$$\text{Standard Gibbs free energy change as: } \Delta G^\circ = -RT \ln k \quad (6)$$

$$\text{and } k = \frac{C_s}{C_e} \quad (7)$$

where ΔG° is the standard Gibbs free energy, ΔH° is the standard enthalpy change, ΔS° is the standard entropy change, T is the absolute temperature (K), k is the adsorption distribution coefficient, C_s is the adsorbed dye concentration at equilibrium (mg L⁻¹), C_e is the remaining dye concentration in solution at equilibrium (mg L⁻¹), and R is the gas constant.

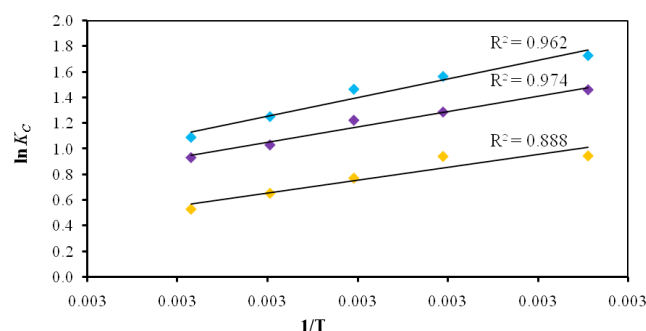


Fig. 6. Van't Hoff plots for the adsorption of CV onto BGW at 100 mg L⁻¹ (◆), 300 mg L⁻¹ (◆) and 500 mg L⁻¹ (◆) CV concentrations [0.050 g of BGW in 25 mL of CV].

Table 4
Thermodynamics parameter values for the adsorption of CV onto BGW

| Conc. (mg L ⁻¹) | ΔH° (kJ mol ⁻¹) | ΔS° (J mol ⁻¹ K ⁻¹) | ΔG° (kJ mol ⁻¹) | | | | | R ² |
|--------------------------------|---|--|--|-------|-------|-------|-------|----------------|
| | | | 298 K | 313 K | 323 K | 333 K | 343 K | |
| 100 | -12.10 | -25.87 | -4.29 | -4.08 | -3.94 | -3.46 | -3.11 | 0.963 |
| 300 | -10.04 | -21.38 | -3.62 | -3.35 | -3.29 | -2.85 | -2.66 | 0.975 |
| 500 | -8.28 | -19.39 | -2.34 | -2.45 | -2.07 | -1.81 | -1.51 | 0.888 |

$$\ln k = \frac{\Delta S^\circ}{R} - \frac{\Delta H^\circ}{RT} \quad (8)$$

Eq. (8) can thus be obtained by substituting Eq. (5) into Eq. (6).

3.6. Investigation of the adsorption kinetics of CV onto BGW

Three different CV dye concentrations were used to understand the kinetics mechanism of the adsorption of CV onto BGW. The experimental data were fitted to two kinetics models: the Lagergren first order [75] and the pseudo second order [76]. Their linear equations are as shown in Table 5. An additional error function *i.e.* Marquardt's percent standard deviation (MPSD) was used and its equation is shown in Eq. (9) below.

$$\text{MPSD: } 100 \sqrt{\frac{1}{p-n} \sum_{i=1}^p (q_{e,meas} - q_{e,calc})^2} \quad (9)$$

From Fig. 7 and Table 6 it is clear that unlike the pseudo second order model which gave R^2 values close to unity for all three dye concentrations, the Lagergren first order gave poor R^2 values. This is further confirmed by the error analyses whereby large error values were observed for the Lagergren first order showing the vast deviation of the calculated values from the experimental data, thus clearly indicates that the kinetics of adsorption of CV on BGW follows the pseudo second order model.

3.7. Regeneration of spent adsorbent and its reusability studies

Spent BGW showed a reduction of 52% at the 5th cycle, while a 23% was observed when it was subjected to washing with distilled water (Fig. 8). Treatment with HCl pro-

Table 5
Linear equations of kinetics models

| Kinetics model | Linear equation | Plot |
|---------------------|---|---------------------------|
| Pseudo first order | $\log(q_e - q_t) = \log(q_e) - \frac{k_1}{2.303} t$ | $\log(q_e - q_t)$ vs. t |
| Pseudo second order | $\frac{t}{q_t} = \frac{q}{k_2 q_e^2} + \frac{1}{q_e} t$ | t/q_t vs. t |

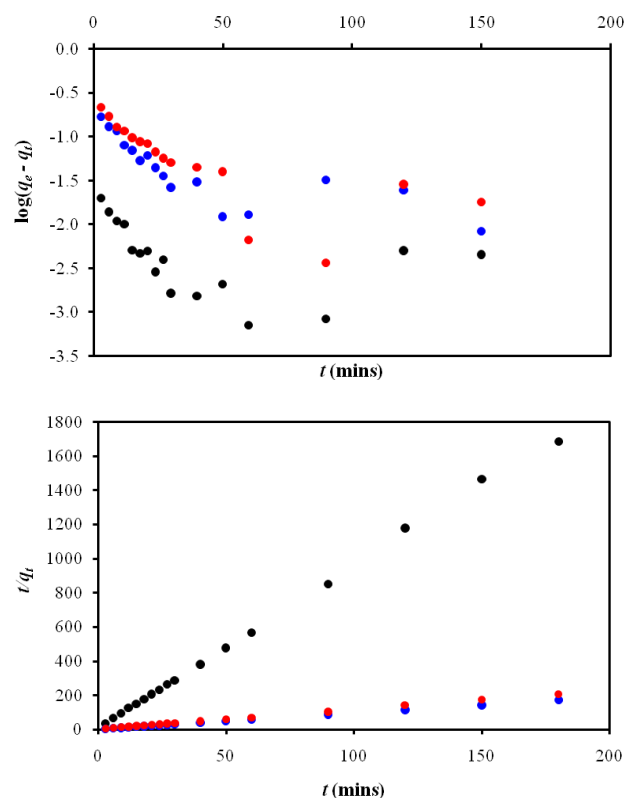


Fig. 7. Linear plots of Lagergren first order (top) and pseudo second order (bottom) models for the adsorption of CV onto BGW at 100 mg L⁻¹ (●), 500 mg L⁻¹ (●) and 700 mg L⁻¹ (●) CV concentrations [mass of BGW = 0.050 g; volume of CV solution = 25 mL].

Table 6

Kinetics parameters and error values for the adsorption of CV onto BGW at different dye concentrations

| Pseudo first order kinetics | | | |
|---|--------|--------|--------|
| Concentration (mg L ⁻¹) | 100 | 500 | 700 |
| ARE | 98.36 | 96.10 | 93.65 |
| SSE | 0.170 | 15.92 | 9.63 |
| HYBRID | 11.12 | 105.3 | 79.73 |
| EABS | 1.70 | 16.44 | 12.78 |
| MPSD | 104.72 | 102.34 | 99.77 |
| χ^2 | 1.67 | 15.80 | 11.96 |
| k_1 (min ⁻¹) | 0.009 | 0.037 | 0.019 |
| R^2 | 0.1559 | 0.8246 | 0.5317 |
| Pseudo second order kinetics | | | |
| Concentration (ppm) | 100 | 500 | 700 |
| ARE | 5.77 | 4.40 | 7.04 |
| SSE | 0.001 | 0.05 | 0.07 |
| HYBRID | 0.07 | 0.34 | 0.61 |
| EABS | 0.09 | 0.74 | 0.94 |
| MPSD | 8.73 | 5.92 | 8.84 |
| χ^2 | 0.01 | 0.05 | 0.09 |
| k_2 (g mmol ⁻¹ min ⁻¹) | 18.73 | 0.834 | 0.649 |
| R^2 | 0.9991 | 0.9999 | 0.9997 |

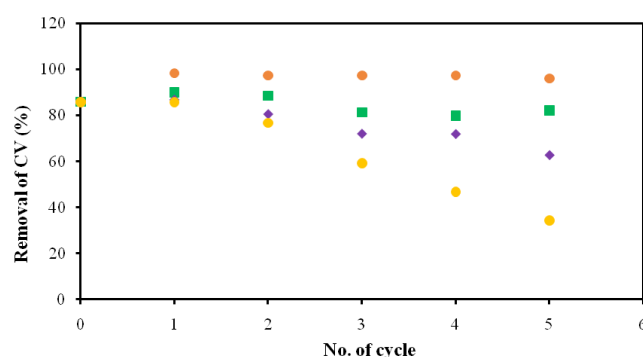


Fig. 8. Regeneration of BGW showing 5 consecutive cycles using different treatment methods: HCl (■), NaOH (●), H₂O (◆) and control (●) [mass of BGW = 0.050 g; concentration of CV = 100 mg L⁻¹].

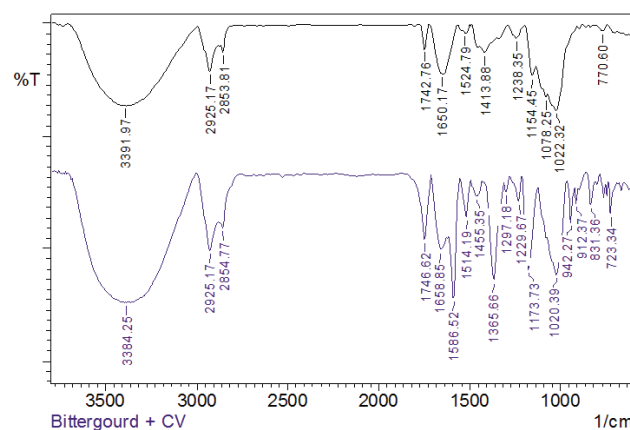


Fig. 9. FTIR spectra for functional group characterization of BGW (top black) and BGW-CV (bottom purple)

vided a good alternative method to regenerate the BGW, where a reduction of 6% was observed at the 4th cycle. Of the methods studied, NaOH treatment was found to be the best. Not only was there no reduction in its ability to remove CV, the adsorbent was found to increase its removal of CV to > 95% and maintaining this percentage removal throughout the 5 cycles.

3.8. Surface morphology and functional group characterization.

There appears to be a distinct difference between the surface morphology of BGW, before and after adsorption of CV dye. In particular, smoothness, and the flat and even in appearance of the adsorbent's surface, were lost during CV adsorption, indicating that the surface of the adsorbent is covered with the dye.

The FTIR spectra recorded (Fig. 9) show shifts in the wavelength of the broad band at around 3,391 to 3384 cm⁻¹ upon adsorption, indicating that hydroxyl group (-OH) and amino acids (N-H) could be involved in the bond formation with dye molecules. Other functional groups that may be involved include alkene (C=C) which shifted from 1650 to

1659 cm^{-1} and also carbonyl group (C=O) where a shift from 1743 to 1747 cm^{-1} was observed. Positive indication of the adsorption of CV on BGW is the appearance of bands of C=C stretch of benzene ring and C–N stretch of aromatic tertiary amine at 1587 cm^{-1} and 1366 cm^{-1} , respectively, as well as the C–N vibration at 1174 cm^{-1} [77].

4. Conclusion

When compared to many reported adsorbents, with its high maximum adsorption capacity of 261.1 mg g^{-1} , based on the Sips isotherm model, bitter melon wastes exhibit great potential as a low-cost adsorbent for the removal of CV dye. Thermodynamics studies indicated that the adsorption process is exothermic and favorable with an increase in orderliness. Pseudo second order kinetics is confirmed by its R^2 value being close to unity. Resilience shown by this adsorbent under various medium pH, coupled with the ability to regenerate and reuse the spent adsorbent under acid or base treatment while maintain high removal of CV adds further value to this adsorbent as a potential low-cost adsorbent for real application in wastewater remediation.

Acknowledgment

The authors thank the Government of Negara Brunei Darussalam, the Universiti Brunei Darussalam, and CAMES for their continuous support.

References

- [1] M.J. Ahmed, Application of agricultural based activated carbons by microwave and conventional activations for basic dye adsorption: review, *J. Environ. Chem. Eng.*, 4 (2016) 89–99.
- [2] M. Rafatullah, O. Sulaiman, R. Hashim, A. Ahmad, Adsorption of methylene blue on low-cost adsorbents: a review, *J. Hazard. Mater.*, 177 (2010) 70–80.
- [3] W.W. Ngah, L. Teong, M. Hanafiah, Adsorption of dyes and heavy metal ions by chitosan composites: A review, *Carbohydr. Polym.*, 83 (2011) 1446–1456.
- [4] T. Zehra, N. Priyantha, L.B.L. Lim, E. Iqbal, Sorption characteristics of peat of Brunei Darussalam V: removal of Congo Red Dye from aqueous solution by peat, *Desal. Water Treat.*, 54 (2015) 2592–2600.
- [5] H.I. Chieng, L.B.L. Lim, N. Priyantha, Sorption characteristics of peat from Brunei Darussalam for the removal of rhodamine B dye from aqueous solution: adsorption isotherms, thermodynamics, kinetics and regeneration studies, *Desal. Water Treat.*, 55 (2015) 664–677.
- [6] N. Priyantha, L.B.L. Lim, S. Wickramasooriya, Adsorption behaviour of Cr (VI) by Muthurajawela peat, *Desal. Water Treat.*, 57 (2016) 16592–16600.
- [7] L.B.L. Lim, N. Priyantha, C.M. Chan, D. Matassan, H.I. Chieng, M.R.R. Kooh, Investigation of the sorption characteristics of Water lettuce (WL) as a potential low-cost biosorbent for the removal of methyl violet 2B, *Desal. Water Treat.*, 57 (2016) 8319–8329.
- [8] E.S. Priya, P.S. Selvan, Water hyacinth (*Eichhornia crassipes*) – An efficient and economic adsorbent for textile effluent treatment – A review, *Arab. J. Chem.*, (2014) doi: 10.1016/j.arabjc.2014.03.002.
- [9] L.B.L. Lim, N. Priyantha, C.M. Chan, D. Matassan, H.I. Chieng, M.R.R. Kooh, Adsorption behavior of Methyl Violet 2B using duckweed: Equilibrium and kinetics studies. *Arab. J. Sci. Eng.*, 39 (2014) 6757–6765.
- [10] T.B. Pushpa, J. Vijayaraghavan, K. Vijayaraghavan, J. Jegan, Utilization of effective microorganisms based water hyacinth compost as biosorbent for the removal of basic dyes, *Desal. Water Treat.*, 57 (2016) 24368–24377.
- [11] N. Priyantha, L.B.L. Lim, M.K. Dahri, Dragon fruit as a potent removal of manganese (II) ions, *J. Appl. Sci. Environ. Sani.*, 8 (2013) 179–188.
- [12] K.M. Al-Qahtani, Water purification using different waste fruit cortexes for the removal of heavy metals, *J. Taibah Uni. Sci.*, 10 (2016) 700–708.
- [13] R. Krishni, K. Foo, B. Hameed, Food cannery effluent, pineapple peel as an effective low-cost biosorbent for removing cationic dye from aqueous solutions, *Desal. Water Treat.*, 52 (2014) 6096–6103.
- [14] S.K. Bajpai, A. Jain, Equilibrium and thermodynamic studies for adsorption of crystal violet onto spent tea leaves (STL), *Water J.*, (2012) doi: 10.14294/WATER.2012.5.
- [15] R. Krishni, K. Foo, B. Hameed, Adsorption of methylene blue onto papaya leaves: comparison of linear and nonlinear isotherm analysis, *Desal. Water Treat.*, 52 (2014) 6712–6719.
- [16] W. Hassan, U. Farooq, M. Ahmad, M. Athar, M.A. Khan, Potential biosorbent, *Haloxylon recurvum* plant stems, for the removal of methylene blue dye, *Arab. J. Chem.*, (2013) doi: 10.1016/j.arabjc.2013.05.002.
- [17] C. Kannan, K. Muthuraja, M.R. Devi, Hazardous dyes removal from aqueous solution over mesoporous aluminophosphate with textural porosity by adsorption, *J. Hazard. Mater.*, 244–245 (2013) 10–20.
- [18] L. Kong, F. Qiu, Z. Zhao, X. Zhang, T. Zhang, J. Pan, D. Yang, Removal of brilliant green from aqueous solutions based on polyurethane foam adsorbent modified with coal, *J. Cleaner Product.*, 137 (2016) 51–59.
- [19] K. Wu, J. Yu, X. Jiang, Multi-walled carbon nanotubes modified by polyaniline for the removal of alizarin yellow R from aqueous solutions, *Adsorp. Sci. Technol.*, (2017) doi/abs/10.1177/0263617416687564.
- [20] A. Mittal, R. Ahmad, I. Hasan, Poly (methyl methacrylate)-grafted alginate/ Fe_3O_4 nanocomposite: synthesis and its application for the removal of heavy metal ions, *Desal. Water Treat.*, 57 (2016) 19820–19833.
- [21] A. Mittal, M. Naushad, G. Sharma, Z.A. Allothman, S.M. Wabaidur, M. Alam, Fabrication of MWCNTs/ ThO_2 nanocomposite and its adsorption behavior for the removal of Pb(II) metal from aqueous medium, *Desal. Water Treat.*, 57 (2016) 21863–21869.
- [22] T. Chinnigounder, M. Shanker, S. Nageswaran, Adsorptive removal of crystal violet dye using agricultural waste Cocoa (*theobroma cacao*) shell, *Res. J. Chem. Sci.*, 1 (2011) 38–45.
- [23] M.H. Baek, C.O. Ijagbemi, S.J. O, D.S. Kim, Removal of malachite green from aqueous solution using degreased coffee bean, *J. Hazard. Mater.*, 176 (2010) 820–828.
- [24] A. Bhatnagar, M. Sillanpää, A. Witek-Krowiak, Agricultural waste peels as versatile biomass for water purification—A review, *Chem. Eng. J.*, 270 (2015) 244–271.
- [25] L. Li, S. Liu, T. Zhu, Application of activated carbon derived from scrap tires for adsorption of Rhodamine B, *J. Environ. Sci.*, 22 (2010) 1273–1280.
- [26] H.A. Hegazi, Removal of heavy metals from wastewater using agricultural and industrial wastes as adsorbents. *HBRC J.*, 9 (2013) 276–282.
- [27] M.A. Adebayo, L.D.T. Prola, E.C. Lima, M.J. Puchana-Rosero, R. Cataluña, C. Saucier, C.S. Umpierrez, J.C.P. Vaghetti, L.G. da Silva, R. Ruggiero, Adsorption of Procion Blue MX-R dye from aqueous solutions by lignin chemically modified with aluminium and manganese, *J. Hazard. Mater.*, 268 (2014) 43–50.
- [28] H. Gao, T. Kan, S. Zhao, Y. Qian, X. Cheng, W. Wu, X. Wang, L. Zheng, Removal of anionic azo dyes from aqueous solution by functional ionic liquid cross-linked polymer, *J. Hazard. Mater.*, 261 (2013) 83–90.
- [29] M. Akgül, Enhancement of the anionic dye adsorption capacity of clinoptilolite by Fe^{3+} -grafting, *J. Hazard. Mater.*, 267 (2014) 1–8.

- [30] S. Behera, S. Das, B. Murmu, R. Mohapatra, T. Sahoo, P. Parhi, Kinetics, thermodynamics and isotherm studies on adsorption of Methyl Violet from aqueous solution using activated bio-adsorbent: phragmites karka, *Current Environ. Eng.*, 3 (2016) 229–241.
- [31] A.H. Jawad, M.A. Islam, B. Hameed, Cross-linked chitosan thin film coated onto glass plate as an effective adsorbent for adsorption of reactive orange 16, *Int. J. Biol. Macromol.*, 95 (2017) 743–749.
- [32] G. Sharma, M. Naushad, D. Pathania, A. Mittal, G.E. El-desoky, Modification of Hibiscus cannabinus fiber by graft copolymerization: application for dye removal, *Desal. Water Treat.*, 54 (2015) 3114–3121.
- [33] M. Naushad, A. Mittal, M. Rathore, V. Gupta, Ion-exchange kinetic studies for Cd(II), Co(II), Cu(II), and Pb(II) metal ions over a composite cation exchanger, *Desal. Water Treat.*, 54 (2015) 2883–2890.
- [34] A. Mittal, R. Ahmad, I. Hasan, Iron oxide-impregnated dextrin nanocomposite: synthesis and its application for the biosorption of Cr(VI) ions from aqueous solution, *Desal. Water Treat.*, 57 (2016) 15133–15145.
- [35] N.V. Boas, J. Casarin, G.P. Gerola, C.R.T. Tarley, J. Caetano, A.C. Gonçalves, D.C. Dragunski, Evaluation of kinetic and thermodynamic parameters in adsorption of lead (Pb²⁺) and chromium (Cr³⁺) by chemically modified macadamia (*Macadamia integrifolia*), *Desal. Water Treat.*, 57 (2016) 17738–17747.
- [36] A. Mittal, M. Teotia, R.K. Soni, J. Mittal, Applications of egg shell and egg shell membrane as adsorbents: A review, *J. Mol. Liq.*, 223 (2016) 376–387.
- [37] A. Mittal, J. Mittal, Hen feather, are markable adsorbent for dye removal. In *Green Chemistry for Dyes Removal from Wastewater*, 2015, pp. 409–457.
- [38] R. Cocampo, S.N. Moreno, The metabolism and mode of action of gentian violet, *Drug Metab. Rev.*, 22 (1990) 161–178.
- [39] A.M. Maley, J.L. Arbiser, Gentian Violet a 19th century drug re-emerges in the 21st century, *Exp. Dermatol.*, 22 (2013) 775–780.
- [40] N.A. Littlefield, B.N. Blackwell, C.C. Hewitt, D.W. Gaylor, Chronic toxicity and carcinogenicity studies of gentian violet in mice, *Fundam. Appl. Toxicol.*, 5 (1985) 902–912.
- [41] R. Docampo, S.N.J. Moreno, The metabolism and mode of action of Gentian Violet, *Drug Metabol. Rev.*, 22 (1990) 161–178.
- [42] P. Drinkwater, Gentian violet—Is it safe? *Australian and New Zealand J. Obs. Gynaecol.*, 30 (1990) 65–66.
- [43] M. Munichandran, B. Gangadhar, G. Naidu, Bioremoval of nickel and lead using bitter gourd (*Momordica charantia*) seeds, *Int. J. Adv. Res. Sci. Eng. Technol.*, 3 (2106) 2475–2484.
- [44] S. Akhtar, A.A. Khan, Q. Husain, Potential of immobilized bitter gourd (*Momordica charantia*) peroxidases in the decolorization and removal of textile dyes from polluted wastewater and dyeing effluent, *Chemosphere*, 60 (2005) 291–301.
- [45] S. Akhtar, Q. Husain, Potential applications of immobilized bitter gourd (*Momordica charantia*) peroxidase in the removal of phenols from polluted water, *Chemosphere*, 65 (2006) 1228–1235.
- [46] Z. Karim, Q. Husain, Removal of anthracene from model wastewater by immobilized peroxidase from *Momordica charantia* in batch process as well as in a continuous spiral-bed reactor, *J. Mol. Catal. B: Enzymatic*, 66 (2010) 302–310.
- [47] M.K. Dahri, M.R.R. Kooh, L.B.L. Lim, Application of *Casuarina equisetifolia* needle for the removal of methylene blue and malachite green dyes from aqueous solution, *Alex. Eng. J.*, 54 (2015) 1253–1263.
- [48] L.B.L. Lim, N. Priyantha, N.A.H. Mohamad Zaidi, A superb modified new adsorbent, *Artocarpus odoratissimus* leaves, for removal of cationic methyl violet 2B dye, *Environ. Earth Sci.*, 75 (2016) 1179.
- [49] H.I. Chieng, N. Priyantha, L.B.L. Lim, Effective adsorption of toxic brilliant green from aqueous solution using peat of Brunei Darussalam: isotherms, thermodynamics, kinetics and regeneration studies, *RSC Adv.*, 5 (2015) 34603–34615.
- [50] M.R.R. Kooh, L.B.L. Lim, M.K. Dahri, L.H. Lim, J.S. Bandara, *Azolla pinnata*: An efficient low cost material for removal of Methyl Violet 2B by using adsorption method, *Waste Biomass Valor.*, 6 (2015) 547–559.
- [51] I. Langmuir, The adsorption of gases on plane surfaces of glass, mica and platinum, *J. Am. Chem. Soc.*, 40 (1918) 1361–1403.
- [52] H. Freundlich, Over the adsorption in the solution, *J. Phys. Chem.*, 57 (1906) 385–470.
- [53] M.M. Dubinin, L.V. Radushkevich, The equation of the characteristic curve of the activated charcoal, *Proc. Acad. Sci. USSR Phys. Chem. Sec.*, 55 (1947) 331–337.
- [54] M.J. Temkin, V. Pyzhev, Kinetics of ammonia synthesis on promoted iron catalyst, *Acta. Physichem. USSR.*, 12 (1940) 327–356.
- [55] O. Redlich, D.L. Peterson, A useful adsorption isotherm, *J. Phys. Chem.*, 63 (1959) 1024–1024.
- [56] R. Sips, Combined form of Langmuir and Freundlich equations, *J. Chem. Phys.*, 16 (1948) 490–495.
- [57] Y.S. Ho, Selection of optimum sorption isotherm, *Carbon*, 42 (2004) 2115–2116.
- [58] D.A. Ratkowsky, D.E. Giles, *Handbook of Nonlinear Regression Models*, M. Dekker New York, 1990.
- [59] L.B.L. Lim, N. Priyantha, N.H.M. Mansor, *Artocarpus altialis* (breadfruit) skin as a potential low-cost biosorbent for the removal of crystal violet dye: equilibrium, thermodynamics and kinetics studies, *Environ. Earth Sci.*, 73 (2015) 3239–3247.
- [60] L.B.L. Lim, N. Priyantha, T. Zehra, C.W. Then, C.M. Chan, Adsorption of crystal violet dye from aqueous solution onto chemically treated *Artocarpus odoratissimus* skin: equilibrium, thermodynamics, and kinetics studies, *Desal. Water Treat.*, 57 (2016) 10246–10260.
- [61] L.B.L. Lim, N. Priyantha, H.H. Cheng, N.A.H.M. Zaidi, Adsorption characteristics of *Artocarpus odoratissimus* leaf toward removal of toxic Crystal violet dye: Isotherm, thermodynamics and regeneration studies, *J. Environ. Biotechnol. Res.*, 4 (2016) 32–40.
- [62] P.D. Saha, S. Chakraborty, S. Chowdhury, Batch and continuous (fixed-bed column) biosorption of crystal violet by *Artocarpus heterophyllus* (jackfruit) leaf powder, *Colloids Surf. B Biointerf.*, 92 (2012) 262–270.
- [63] H.I. Chieng, L.B.L. Lim, N. Priyantha, Enhancement of crystal violet dye adsorption on *Artocarpus camansi* peel through sodium hydroxide treatment, *Desal. Water Treat.*, 58 (2017) 320–331.
- [64] T. Zehra, N. Priyantha, L.B.L. Lim, Removal of crystal violet dye from aqueous solution using yeast-treated peat as adsorbent: thermodynamics, kinetics, and equilibrium studies, *Environ. Earth Sci.*, 75 (2016) 1–15.
- [65] L.B.L. Lim, N. Priyantha, H.H. Cheng, N.A.H.M. Zaidi, *Parkia speciosa* (Petai) pod as a potential low-cost adsorbent for the removal of toxic crystal violet dye, *Scientia Bruneiana Special Iss.*, 15 (2016) 99–106.
- [66] M. Baghdadi, A. Jafari, A. Pardakhti, Removal of crystal violet from aqueous solutions using functionalized cellulose microfibers: a beneficial use of cellulosic healthcare waste, *RSC Adv.*, 6 (2016) 61423–61433.
- [67] M.E.K. Noureddine El Messaoudi, S. Bentahar, A. Dbik, A. Lacherai, Removal of crystal violet by biosorption onto date stones, *Sci. Study Res.*, 17 (2016) 151–167.
- [68] T.D.R. Aydogmus, M. Sarikaya, A.R. Kul, Y. Onal, Adsorption of Crystal Violet on activated carbon prepared from coal flotation concentrate, *IOP Conf. Ser.: Earth Environ. Sci.*, 44 (2016) 052022.
- [69] M.A. Atallah, M.A. Al-Ghobashy, M. Nebsen, M.Y. Salem, Removal of cationic and anionic dyes from aqueous solution with magnetite/pectin and magnetite/silica/pectin hybrid nanocomposites: kinetic, isotherm and mechanism analysis, *RSC Adv.*, 6 (2016) 11461–11480.
- [70] H.I. Chieng, L.B.L. Lim, N. Priyantha, D.T.B. Tennakoon, Sorption characteristics of peat of Brunei Darussalam III: equilibrium and kinetics studies on adsorption of Crystal Violet (CV), *Int. J. Earth. Sci. Eng.*, 6 (2013) 791–801.
- [71] R. Ahmad, Studies on adsorption of crystal violet dye from aqueous solution onto coniferous pinus bark powder (CPBP), *J. Hazard. Mater.*, 171 (2009) 767–773.

- [72] A. Oladipo, M. Gazi, Enhanced removal of crystal violet by low cost alginate/acid activated bentonite composite beads: Optimization and modelling using non-linear regression technique, *J. Water. Process. Eng.*, 2 (2014) 43–52.
- [73] A. Saeed, M. Sharif, M. Iqbal, Application potential of grapefruit peel as dye sorbent: Kinetics, equilibrium and mechanism of crystal violet adsorption, *J. Hazard. Mater.*, 179 (2010) 564–572.
- [74] S.K. Ghosh, A. Bandyopadhyay, Characterizing acidic fly ash with and without biomass combustion residue for adsorptive removal of crystal violet with optimization of mixed adsorbent by response surface modeling, *Environ. Earth Sci.*, 75 (2016) 820.
- [75] S. Lagergren, About the theory of so-called adsorption of soluble substances, *K. Sven. Vetenskapsakad. Handl.*, 24 (1898) 1–39.
- [76] Y.S. Ho, G. McKay, Sorption of dye from aqueous solution by peat, *Chem. Eng. J.*, 70 (1998) 115–124.
- [77] J. Cheriaa, M. Khairredine, M. Rouabhia, A. Bakhrouf, Removal of triphenylmethane dyes by bacterial consortium, *The Sci. World J.*, 2012 (2012) Article ID 512454.